Nanoscale

COMMUNICATION

View Article Online
View Journal | View Issue

Cite this: *Nanoscale*, 2014, **6**, 12345

Received 23rd June 2014,
Accepted 17th August 2014

DOI: 10.1039/c4nr03490b

www.rsc.org/nanoscale

Mercaptopropionic acid-capped Mn^{2+}:ZnSe/ZnO quantum dots with both downconversion and upconversion emissions for bioimaging applications†

Bingxia Zhao,‡[a] Yulian Yao,‡[a] Kai Yang,[b] Pengfei Rong,[c] Peng Huang,[c] Kang Sun,*[a] Xiao An,[d] Zhiming Li,[e] Xiaoyuan Chen[c] and Wanwan Li*[a]

Doped quantum dots (d-dots) can serve as fluorescent biosensors and biolabels for biological applications. Our study describes a synthesis of mercaptopropionic acid (MPA)-capped Mn^{2+}:ZnSe/ZnO d-dots through a facile, cost-efficient hydrothermal route. The as-prepared water-soluble d-dots exhibit strong emission at *ca.* 580 nm, with a photoluminescence quantum yield (PLQY) as high as 31%, which is the highest value reported to date for such particles prepared *via* an aqueous route. They also exhibit upconversion emission when excited at 800 nm. With an overall diameter of around 6.7 nm, the d-dots could gain access to the cell nucleus without any surface decoration, demonstrating their promising broad applications as fluorescent labels.

Quantum dots (QDs) or semiconductor nanocrystals are of great interest to fundamental studies and potential applications as fluorescent probes, fluorescent biosensors, light-emitting diodes (LEDs), and solar cells.[1–6] Recently, introducing transition metal ions into the intrinsic QDs has been widely explored because of the unique optical properties of the d-dots.[7–11] The d-dots not only retain nearly all the advantages of intrinsic QDs but also possess new properties such as the enhancement of the thermal stability, the reduction of the chemical sensitivity, and the elimination of the self-quenching and re-absorption due to enlarged Stokes shift caused by absorption/energy transfer. Mn^{2+}:ZnSe QD is one of the most popular d-dots because of its cadmium free, remarkable magneto-optical properties and the long fluorescence lifetime of the Mn^{2+} emission suitable for broad applications.[11–19]

Although numerous organometallic routes were reported to successfully synthesize oil-soluble Mn^{2+}:ZnSe QDs with high PLQYs in the last decade,[11–15] direct synthesis of highly fluorescent Mn^{2+}:ZnSe QDs in aqueous medium is still a challenge. A typical approach to prepare aqueous d-dots requires at least two steps (nucleation and growth) and hours of refluxing to achieve the optimal optical properties,[17–20] and the PLQYs of the most as-prepared aqueous d-dots are less than 5%, which greatly limits their applications. Although ZnS or ZnO shells can be coated around MPA or 1-thioglycerol (TG) stabilized d-dots to improve their PLQYs, the coating procedure is also time-consuming, and the PLQYs of the resulting core/shell d-dots are still less than 15%. Therefore, it is of significance and is a great challenge to develop an effective route to prepare highly fluorescent Mn^{2+}:ZnSe QDs in aqueous solution.

In this Communication, we successfully synthesized MPA stabilized Mn^{2+}:ZnSe/ZnO d-dots through the hydrothermal route for the first time (see Scheme 1), which is considered as

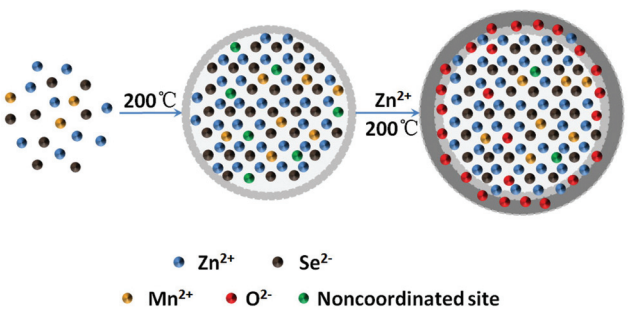

Scheme 1 Schematic representation of the synthesis of MPA-Mn^{2+}:ZnSe/ZnO d-dots.

[a]*State Key Lab of Metal Matrix Composites, School of Materials Science and Engineering, Shanghai Jiao Tong University, 800 Dongchuan Road, Shanghai 200240, P. R. China. E-mail: wwli@sjtu.edu.cn, ksun@sjtu.edu.cn*
[b]*School of Radiation Medicine and Protection (SRMP) and School of Radiological and Interdisciplinary Sciences (RAD-X), Soochow University, Suzhou, Jiangsu 215123, P. R. China*
[c]*Laboratory of Molecular Imaging and Nanomedicine (LOMIN), National Institute of Biomedical Imaging and Bioengineering (NIBIB), National Institutes of Health (NIH), Bethesda, MD 20892, USA*
[d]*The First People's Hospital Affiliated to Shanghai Jiao Tong University School of Medicine, 100 Haining Road, Shanghai 200080, P. R. China*
[e]*Department of Dermatology and Venereology, the First Affiliated Hospital of Wenzhou Medical University, Wenzhou, Zhejiang 325000, P. R. China*
†Electronic supplementary information (ESI) available: Experimental details, characterization and cell culture tests results. See DOI: 10.1039/c4nr03490b
‡These authors contributed equally to this work.

a simple and highly efficient method. One-step process was used to prepare Mn^{2+}:ZnSe d-dots by simply mixing the dopant and the host precursor together and heating the mixture in a Teflon-lined stainless autoclave for less than 1 hour; the resulting d-dots exhibited PLQY of 12.5%. Then a ZnO shell was successfully coated onto the as-prepared d-dots hydrothermally, resulting in an improved PLQY up to 19.8%. Moreover, we found that photoactivation post-treatment was an effective way to further improve their PLQY irreversibly, which can reach up to 31% after 8 W 365 nm UV lamp irradiation for about 4 hours, the highest reported value of water-soluble Mn^{2+}:ZnSe/ZnO d-dots *via* the aqueous route so far.

Fig. 1a demonstrates the UV-vis absorption and PL spectra of Mn^{2+}:ZnSe d-dots at different reaction times during the one-step hydrothermal synthesis. An obvious red shift of absorption and the PL peak toward longer wavelength could be observed with prolonged reaction time, together with a gradual decrease of the intensity of the bandgap PL corresponding to the ZnSe QDs centered at about 400 nm, trap state emission from surface defects at about 460 nm, and a gradual increase of the intensity of the pseudo-tetrahedral ($^4T_1$ to $^6A_1$) transition of Mn^{2+} ions incorporated into the ZnSe QDs at about 570 nm. As Peng *et al.*[11] have claimed, Mn^{2+} is a harder Lewis acid than Zn^{2+}, which should be significantly less reactive than Zn^{2+} if they both have the same carboxylate ligand. Thus, in our one-step strategy, it is quite possible that the ZnSe crystals were firstly formed followed by the absorbance of the dopants onto the surface. As the reaction continued, more Mn^{2+} ions were incorporated into the ZnSe crystal by replacing the Zn element. As the internal doping continued, the intensity of trap emission and band gap emission gradually decreased and the $^4T_1$ to $^6A_1$ emission of Mn^{2+} became dominant. Finally, only the $^4T_1$ to $^6A_1$ emission of Mn^{2+} remained in the Mn^{2+}:ZnSe d-dots. In our experiments, "growth-doping" was realized by a one-pot procedure, which was much more convenient, time-saving and suitable for large scale fabrication, and cubic zinc blended Mn^{2+}:ZnSe d-dots with PLQY up to 12.5% and the average diameter of about 3 nm (Fig. 1b) can be prepared at 200 °C in 30 min.

Although the as-prepared Mn^{2+}:ZnSe d-dots possess PLQY comparable to the core/shell d-dots prepared through other aqueous routes,[17–22] the PLQY of 12.5% is still not ideal for further applications. Therefore, Mn^{2+}:ZnSe/ZnO core/shell QDs were synthesized to further improve both the chemical stability and PLQY of Mn^{2+}:ZnSe QDs. ZnO was chosen as the shell material due to its wide band gap (3.37 eV at room temperature), which is also believed to be non-toxic and bio-safe.[23] Unlike the synthesis of core/shell QDs from organic solution, it is much more difficult to prepare water-soluble core/shell QDs from aqueous solution due to the complex solution environment. It is reported that the epitaxial growth of the ZnO shell is achieved by adding Zn^{2+} salt to the d-dots solution under alkaline conditions, and the added Zn^{2+} would be hydrolyzed into $Zn(OH)_2$ which would then dehydrate into ZnO and deposit onto the surface of QDs and form a ZnO shell. However, it was claimed that hydrothermal conditions are not suitable for ZnO shell coating, and the QDs would aggregate and thus capping could not be achieved.[24] In our experiments, a hydrothermal route was applied instead of the refluxing to successfully obtain the core/shell structure rapidly, and an excess amount of MPA (ZnSe : MPA = 1 : 3.6) was used in the synthesis to avoid aggregation. The ZnO shell was successfully installed onto the Mn^{2+}:ZnSe d-dots (see Fig. 2b, Fig. S1 and Table S1†) to obtain the MPA-capped Mn^{2+}:ZnSe/

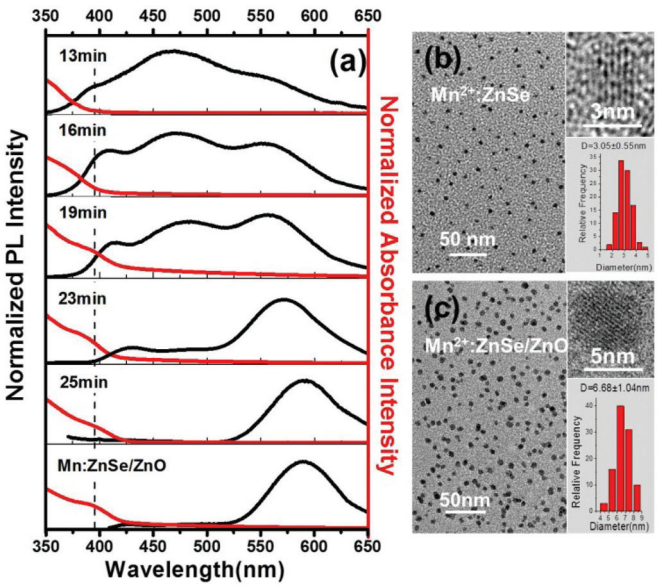

Fig. 1 (a) Evolution of ultraviolet–visible (UV–vis) absorption and PL spectra of MPA-Mn^{2+}:ZnSe d-dots with the reaction time and the UV–vis absorption and PL spectra of MPA-Mn^{2+}:ZnSe/ZnO d-dots. TEM and HRTEM of MPA-Mn^{2+}:ZnSe d-dots (b) and MPA-Mn^{2+}:ZnSe/ZnO d-dots (c).

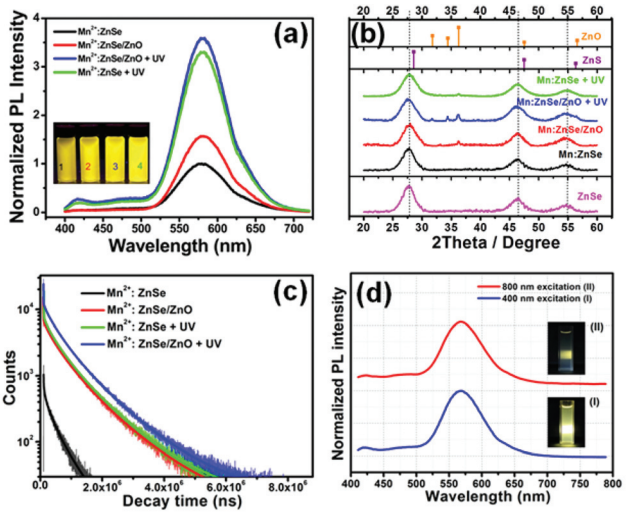

Fig. 2 (a) PL spectra variation and (b) XRD patterns and (c) decay curves of MPA-Mn^{2+}:ZnSe and MPA-Mn^{2+}:ZnSe/ZnO d-dots before and after 365 nm UV light irradiation. (d) PL spectra of MPA-Mn^{2+}:ZnSe/ZnO d-dots excited by 400 nm and 800 nm. The inserts are photographs of the d-dots excited by 400 nm (I) and 800 nm (II).

ZnO d-dots with an average diameter of ~6.7 nm (see Fig. 1c), and their PLQY was improved up to 19.8% in 15 min (see Fig. 2a). No change in the PL peak position was observed before and after ZnO shell coating (see Fig. 1a), which was also observed in other reports when overcoating uncapped ZnS:Mn or ZnSe:Mn nanocrystals with a ZnO shell.[21,25]

As the hyperfine splitting is strongly dependent on the local environment, the EPR test was carried out to determine the locality and distribution of Mn^{2+} ions in the d-dots. A typical EPR spectrum of the Mn^{2+}:ZnSe/ZnO d-dots is shown in Fig. S2.† Differently from the classic six-line hyperfine splitting pattern of Mn^{2+}, the EPR signal of the Mn^{2+}:ZnSe/ZnO d-dots appears as a broad line feature, which is similar to that of aqueous synthesized Mn^{2+}:ZnSe QDs.[19] The broad line feature indicated that a high concentration of Mn^{2+} was doped into the ZnSe QDs and the strong dipolar interactions between Mn^{2+}–Mn^{2+} influenced the hyperfine splitting of the EPR signal.[26,27]

The photostability of the as-prepared d-dots was evaluated (as shown in Fig. S3†), and an interesting phenomenon was observed that the PLQY of the d-dots would increase gradually under 8 W 365 nm UV lamp irradiation and could reach up to 31% after about 4 h irradiation (see Fig. 2a), which is much higher than those reported in other literature reports.[17–22] It has been reported that the PLQY enhancement of MPA-capped Mn^{2+}:ZnSe in some situations could result from the forming of the ZnS shell.[28] We, however, found that the wurtzite structure of ZnO could either emerge or could be better crystallized for Mn^{2+}:ZnSe or Mn^{2+}:ZnSe/ZnO respectively under UV irradiation for a certain time (see Fig. 2b). We did not observe obvious particle size variation of Mn^{2+}:ZnSe or Mn^{2+}:ZnSe/ZnO d-dots after UV irradiation. It was reported that some molecules would be adsorbed on the surface of the quantum dots under UV irradiation.[29–31] Some of the adsorbed molecules could be removed by simply turning the illumination source off. The other adsorbed molecules, however, would form an oxide layer irreversibly. A ZnO shell, therefore, could form under UV irradiation for a period of time (see Fig. 2b), which resulted in a great improvement of the PLQY of Mn^{2+}:ZnSe d-dots comparable to that of Mn^{2+}:ZnSe/ZnO d-dots. However, the hydrothermally synthesized Mn^{2+}:ZnSe/ZnO d-dots under UV irradiation could achieve the highest PLQY in a much shorter time than that of the direct irradiated Mn^{2+}:ZnSe d-dots (see Fig. S3†). Moreover, the thermal stabilities of Mn^{2+}:ZnSe and Mn^{2+}:ZnSe/ZnO d-dots were also improved after 365 nm UV irradiation, and the irradiated Mn^{2+}:ZnSe/ZnO d-dots showed excellent thermal stability (see Fig. S4†), which is good for their further applications. pH stability of Mn^{2+}:ZnSe and Mn^{2+}:ZnSe/ZnO d-dots was also measured to insure their bio-application. The pH value was adjusted to 5.5 and 7.4, corresponding to the pH of lysosomal and serum respectively. As is shown in Fig. S5,† the PL intensity would decrease to some degree under low pH environment, which could still maintain over 70% of their initial value for the Mn^{2+}:ZnSe/ZnO core/shell d-dots. The low-pH stability of the Mn^{2+}:ZnSe/ZnO d-dots is better than that of Mn^{2+}:ZnSe d-dots, indicating that the ZnO could improve the chemical stability of d-dots.

The crystal structure of the prepared d-dots could be confirmed by the powder XRD patterns. As shown in Fig. 2b, all the nanocrystals of Mn^{2+}:ZnSe and Mn^{2+}:ZnSe/ZnO before and after 8 W 365 nm UV lamp irradiation exhibit characteristic peaks at about 27.5°, 45.6°, and 54.3° corresponding to the (111), (220), and (311) reflecting planes of cubic zinc blended ZnSe. No obvious shift could be seen between the Mn^{2+}:ZnSe and Mn^{2+}:ZnSe/ZnO,[21] indicating that the capping shell was not a ZnS and the ZnO shell does not change the lattice spacing of ZnSe nanocrystals. Different from the other reports,[21,24] the emergence of the ZnO wurtzite phase could be observed while there was no obvious further shift of the characteristic peaks to higher angle, indicating that the enhancement of PLQY is not related to the formation of ZnS layers as described in the literature.[28] Though the ZnO shell could be installed either by the UV irradiation or thermally, the ZnO wurtzite phase of thermally synthesized Mn^{2+}:ZnSe/ZnO d-dots was much clearer than that of the direct UV irradiated ones, implying that the direct UV treatment could only result in the formation of a very thin ZnO shell, while the ZnO shell could be thicker (see Fig. 1c) and better crystallized in the hydrothermal route, and a 365 nm UV treatment on the hydrothermally synthesized Mn^{2+}:ZnSe/ZnO could make the ZnO shell further crystallized (see Fig. 2b). Moreover, the formation of ZnO layers around Mn:ZnSe d-dots could also be confirmed by measuring the PL decay of the d-dots (see Fig. 2c and Table S2†), and the Mn^{2+} ion emission lifetime of Mn^{2+}:ZnSe d-dots is much shorter than that of UV irradiated Mn^{2+}:ZnSe, Mn^{2+}:ZnSe/ZnO and UV irradiated Mn^{2+}:ZnSe/ZnO d-dots. It is reported that the Mn^{2+} ion emission lifetime is dependent on the diameter of the nanocrystals and is longer for d-dots with a thicker overcoating layer or thicker diffusion region.[17,32] The longer decay times of the core/shell d-dots, attributed to the emission of the single isolated Mn^{2+} ions in a cubic site,[33–35] provide another evidence of the deeper embedding of Mn^{2+} dopant centers in these d-dots. It is worth noting that the emission lifetime of MPA-Mn^{2+}:ZnSe/ZnO d-dots after UV irradiation can reach up to 902 μs, which could be utilized for time-resolved fluorescence detection.[36,37]

It is also interesting that the as-prepared MPA-Mn^{2+}:ZnSe/ZnO d-dots show upconversion fluorescence properties and can be excited by an 800 nm laser (see Fig. 2d and Fig. S6†). The emission spectra and the corresponding emission photographs excited by 400 nm and 800 nm lasers are displayed in Fig. 2d. The emission peaks which were excited by the 800 nm laser matched well with their respective counterparts under 400 nm UV excitation. Strong up-conversion luminescence of Mn^{2+} in Mn^{2+}:ZnS nanoparticles is attributed to a two-photon absorption process,[38] in which one nanocrystal simultaneously absorbs two photons, whose sum energy is equal to the energy difference between the conductive band and the valence band. Due to the similar crystal structure and the same doping ions, the up-conversion luminescence of Mn^{2+} in the as-prepared Mn^{2+}:ZnSe d-dots might also be attributed to the two-photon absorption process, suggesting their applications in bio-

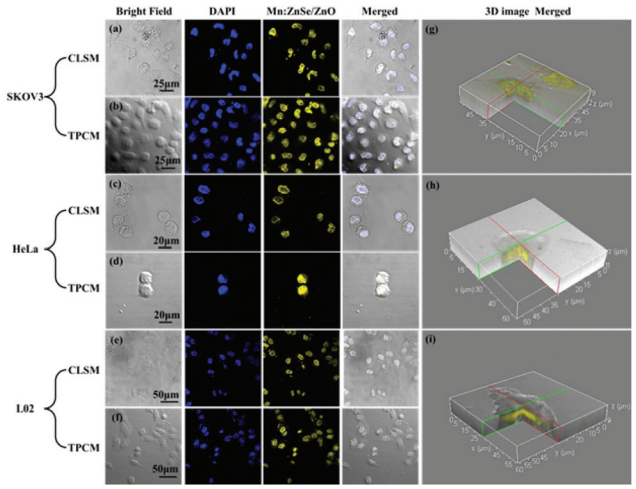

Fig. 3 The confocal laser scanning microscopy (CLSM) images and two photon confocal microscopy (TPCM) images of SKOV3 cells (a), (b); HeLa cells (c), (d); L02 cells (e), (f) cultured in MPA-Mn^{2+}:ZnSe/ZnO d-dots solution. The left boxes correspond to bright field images, fluorescence images (DAPI and d-dots) are shown in the middle, and the right ones show overlays of the bright field and fluorescence images. Two photon microscopy images were obtained with laser excitation at 800 nm. (g), (h), (i) are reconstructed 3D images (overlays of the bright field and d-dots fluorescence images) from Z-stack sections of 2D CLSM images of SKOV3, HeLa and L02 cells respectively.

imaging excited by multiphotons of the near-infrared region. Recently, multiphoton bioimaging has attracted much attention due to little near-infrared absorption from endogenous species and water.[39,40]

The synthesized MPA-Mn^{2+}:ZnSe/ZnO d-dots are expected to show low cytotoxicity. Fig. S7† displays the cell viability of SKOV3, HeLa and L02 cells in the presence of MPA-Mn^{2+}:ZnSe/ZnO d-dots suspension, and the d-dots exhibited low cytotoxicity (greater than 80% cell viability, <200 μg mL^{-1}) and were slightly affected at higher concentrations (400 μg mL^{-1}). The confocal laser scanning microscopy (CLSM) images (Fig. 3a, c and e) show SKOV3, HeLa and L02 cells labeled with MPA-Mn^{2+}:ZnSe/ZnO d-dots under 400 nm excitation. The yellow emission was clearly observed from all three kinds of cells. The multi-photon cell labeling of MPA-Mn^{2+}:ZnSe/ZnO d-dots was also demonstrated using SKOV3, HeLa and L02 cells. As shown in Fig. 3b, d and f, strong yellow emission from the cells was detected under the excitation of the 800 nm laser. These results suggested that the obtained MPA-Mn^{2+}:ZnSe/ZnO d-dots showed promising cell labeling applications under either UV or near infrared excitations.

Notably, both the confocal laser scanning microscopy (CLSM) and two photon confocal microscopy (TPCM) images showed that MPA-Mn^{2+}:ZnSe/ZnO d-dots had a strong affinity for cell nuclei (Fig. 3a–f). The fluorescent d-dots were highly concentrated in the nuclei of SKOV3, HeLa and L02 cells. To further investigate the location of the d-dots, Z-stack sections of 2D CLSM images of SKOV3, HeLa and L02 cells stained by MPA-Mn^{2+}:ZnSe/ZnO d-dots were reconstructed into 3D images for observation (see Fig. 3e–g, Fig. S8 and Movie S1†). The 3D CLSM images clearly showed that MPA-Mn^{2+}:ZnSe/ZnO d-dots were preferentially concentrated in the cell nuclei. Bio-TEM pictures of MPA-Mn^{2+}:ZnSe/ZnO stained HeLa cells were also taken (see Fig. S9†). It could be obviously seen in Fig. S9a† that the MPA-Mn^{2+}:ZnSe/ZnO d-dots were located mainly in the cell nucleus. However, the d-dots were separated randomly in the nucleus, and there was no specific location for them (see Fig. S9b†). Because of the importance of visualizing cell nuclei, many selective nuclei staining techniques, including NoLS polypeptides and antibodies to specific proteins,[41,42] and those that target the genetic materials (DNA or RNA) were reported.[43,44] However, it is a complicated case for nucleus-targeting QDs, and both suitable size for cell permeability and specific interaction with nucleus materials are important for QDs to achieve the nucleus-targeting function. At physiological pH, the negatively charged MPA-Mn^{2+}:ZnSe/ZnO d-dots might bind to positively charged basic proteins, such as histone, which are abundant in cell nuclei, and may be the driving force of the nucleus-targeting functions of MPA-Mn^{2+}:ZnSe/ZnO d-dots. However, the size of MPA-Mn^{2+}:ZnSe/ZnO d-dots is about 6.7 nm, which is much bigger than that of the reported nucleus-targeting QDs (glutathione (GSH)-capped CdTe (4.0 nm),[45] thioglycolic acid (TGA)-capped CdTe (3.6 and 2.6 nm)[46] and 1,2,3-triazole-PEG (TA)-capped CdS (<4.0 nm)[47]). A detailed study of the nucleus-targeting functions of MPA-Mn^{2+}:ZnSe/ZnO d-dots will be carried out in the future.

In summary, our study describes a synthesis of mercaptopropionic acid (MPA)-capped Mn^{2+}:ZnSe/ZnO d-dots through a facile hydrothermal route that is cost-effective. The as-prepared water-soluble d-dots exhibit strong emission at a wavelength of about 580 nm with the quantum yield as high as 31%, which is the highest reported value *via* the aqueous route so far. They also exhibit upconversion emission at the excitation of 800 nm. With an overall size as big as ~6.7 nm, they could surprisingly gain access to the cell nucleolus, demonstrating their promising broad applications as fluorescent labels.

Acknowledgements

This work was financially supported by the National Basic Research Program of China (973 program, 2010CB933901, 2013CB733802), the National Natural Science Foundation of China (project no. 50902093, 81272987, 81371645), a grant to Prof. Wanwan Li from the Ph.D. Programs Foundation of the Ministry of Education of China (project no. 200802481131), Medicine & Engineering Cross Research Foundation of Shanghai Jiao Tong University (project no. YG2012MS61), and Zhejiang Provincial Natural Science Foundation of China (project no. LY12H11011). We thank the Instrumental Analysis Center of SJTU for the assistance with TEM, XRD and XPS characterization.

Notes and references

1 X. Gao, Y. Cui, R. M. Levenson, L. W. Chung and S. Nie, *Nat. Biotechnol.*, 2004, **22**, 969–976.
2 M. Han, X. Gao, J. Z. Su and S. Nie, *Nat. Biotechnol.*, 2001, **19**, 631.
3 J. Lim, S. Jun, E. Jang, H. Baik, H. Kim and J. Cho, *Adv. Mater.*, 2007, **19**, 1927–1932.
4 Y. Q. Li, A. Rizzo, R. Cingolani and G. Gigli, *Adv. Mater.*, 2006, **18**, 2545–2548.
5 A. J. Nozik, *Physica E*, 2002, **14**, 115–120.
6 A. M. Smith, H. Duan, A. M. Mohs and S. Nie, *Adv. Drug Delivery Rev.*, 2008, **60**, 1226–1240.
7 S. C. Erwin, L. Zu, M. I. Haftel, A. L. Efros, T. A. Kennedy and D. J. Norris, *Nature*, 2005, **436**, 91–94.
8 J. W. Stouwdam and R. A. J. Janssen, *Adv. Mater.*, 2009, **21**, 2916–2920.
9 X. Wang, X. Yan, W. Li and K. Sun, *Adv. Mater.*, 2012, **24**, 2742–2747.
10 P. Wu and X. P. Yan, *Chem. Soc. Rev.*, 2013, **42**, 5489–5521.
11 N. Pradhan, D. Goorskey, J. Thessing and X. Peng, *J. Am. Chem. Soc.*, 2005, **127**, 17586–17587.
12 R. Zeng, M. Rutherford, R. Xie, B. Zou and X. Peng, *Chem. Mater.*, 2010, **22**, 2107–2113.
13 R. Zeng, T. Zhang, G. Dai and B. Zou, *J. Phys. Chem. C*, 2011, **115**, 3005–3010.
14 H. Shen, H. Wang, X. Li, J. Z. Niu, X. Chen and L. S. Li, *Dalton Trans.*, 2009, 10534–10540.
15 N. Pradhan and D. D. Sarma, *J. Phys. Chem. Lett.*, 2011, **2**, 2818–2826.
16 N. Pradhan, D. M. Battaglia, Y. Liu and X. Peng, *Nano Lett.*, 2006, **7**, 312–317.
17 A. Aboulaich, M. Geszke, L. Balan, J. Ghanbaja, G. Medjahdi and R. Schneider, *Inorg. Chem.*, 2010, **49**, 10940–10948.
18 J. a. Liu, X. Wei, Y. Qu, J. Cao, C. Chen and H. Jiang, *Mater. Lett.*, 2011, **65**, 2139–2141.
19 C. Wang, X. Gao, Q. Ma and X. Su, *J. Mater. Chem.*, 2009, **19**, 7016–7022.
20 P. Shao, Q. Zhang, Y. Li and H. Wang, *J. Mater. Chem.*, 2011, **21**, 151.
21 A. Aboulaich, L. Balan, J. Ghanbaja, G. Medjahdi, C. Merlin and R. l. Schneider, *Chem. Mater.*, 2011, **23**, 3706–3713.
22 X. Gao, H. Zhang, Y. Li and X. Su, *Anal. Bioanal. Chem.*, 2012, **402**, 1871–1877.
23 D. V. Talapin, J.-S. Lee, M. V. Kovalenko and E. V. Shevchenko, *Chem. Rev.*, 2009, **110**, 389–458.
24 F. Aldeek, L. Balan, G. Medjahdi, T. Roques-Carmes, J.-P. Malval, C. Mustin, J. Ghanbaja and R. l. Schneider, *J. Phys. Chem. C*, 2009, **113**, 19458–19467.
25 D. Jiang, L. Cao, W. Liu, G. Su, H. Qu, Y. Sun and B. Dong, *Nanoscale Res. Lett.*, 2009, **4**, 78–83.
26 T. J. Norman, D. Magana, T. Wilson, C. Burns, J. Z. Zhang, D. Cao and F. Bridges, *J. Phys. Chem. B*, 2003, **107**, 6309–6317.
27 P. A. Gonzalez Beermann, B. R. McGarvey, S. Muralidharan and R. C. Sung, *Chem. Mater.*, 2004, **16**, 915–918.
28 G.-Y. Lan, Y.-W. Lin, Y.-F. Huang and H.-T. Chang, *J. Mater. Chem.*, 2007, **17**, 2661.
29 S. R. Cordero, P. J. Carson, R. A. Estabrook, G. F. Strouse and S. K. Buratto, *J. Phys. Chem. B*, 2000, **104**, 12137–12142.
30 S. Dembski, C. Graf, T. Kruger, U. Gbureck, A. Ewald, A. Bock and E. Ruhl, *Small*, 2008, **4**, 1516–1526.
31 C. Carrillo-Carrion, S. Cardenas, B. M. Simonet and M. Valcarcel, *Chem. Commun.*, 2009, 5214–5226.
32 C. Gan, Y. Zhang, D. Battaglia, X. Peng and M. Xiao, *Appl. Phys. Lett.*, 2008, **92**, 241111.
33 A. A. Bol and A. Meijerink, *Phys. Rev. B: Condens. Matter*, 1998, **58**, R15997–R16000.
34 B. A. Smith, J. Z. Zhang, A. Joly and J. Liu, *Phys. Rev. B: Condens. Matter*, 2000, **62**, 2021–2028.
35 J. Zheng, X. Yuan, M. Ikezawa, P. Jing, X. Liu, Z. Zheng, X. Kong, J. Zhao and Y. Masumoto, *J. Phys. Chem. C*, 2009, **113**, 16969–16974.
36 D. Zhu, Y. Chen, L. Jiang, J. Geng, J. Zhang and J. J. Zhu, *Anal. Chem.*, 2011, **83**, 9076–9081.
37 H.-F. Wang, Y. He, T.-R. Ji and X.-P. Yan, *Anal. Chem.*, 2009, **81**, 1615–1621.
38 W. Chen, A. Joly and J. Zhang, *Phys. Rev. B: Condens. Matter*, 2001, **64**, 041202.
39 L. Cao, X. Wang, M. J. Meziani, F. Lu, H. Wang, P. G. Luo, Y. Lin, B. A. Harruff, L. M. Veca, D. Murray, S.-Y. Xie and Y.-P. Sun, *J. Am. Chem. Soc.*, 2007, **129**, 11318–11319.
40 L. M. Maestro, E. M. n. Rodríguez, F. S. Rodríguez, M. C. I.-d. la Cruz, A. Juarranz, R. Naccache, F. Vetrone, D. Jaque, J. A. Capobianco and J. G. a. Solé, *Nano Lett.*, 2010, **10**, 5109–5115.
41 K. A. Dean, O. von Ahsen, D. Görlich and H. M. Fried, *J. Cell Sci.*, 2001, **114**, 3479–3485.
42 C. Korgaonkar, J. Hagen, V. Tompkins, A. A. Frazier, C. Allamargot, F. W. Quelle and D. E. Quelle, *Mol. Cell. Biol.*, 2005, **25**, 1258–1271.
43 X. Liu, H. Chen and D. Patel, *J. Biomol. NMR*, 1991, **1**, 323–347.
44 Q. Li, Y. Kim, J. Namm, A. Kulkarni, G. R. Rosania, Y.-H. Ahn and Y.-T. Chang, *Chem. Biol.*, 2006, **13**, 615–623.
45 Y. Zheng, S. Gao and J. Y. Ying, *Adv. Mater.*, 2007, **19**, 376–380.
46 Y. Williams, A. Sukhanova, M. Nowostawska, A. M. Davies, S. Mitchell, V. Oleinikov, Y. Gun'ko, I. Nabiev, D. Kelleher and Y. Volkov, *Small*, 2009, **5**, 2581–2588.
47 R. Shen, X. Shen, Z. Zhang, Y. Li, S. Liu and H. Liu, *J. Am. Chem. Soc.*, 2010, **132**, 8627–8634.